

Adaptive independent component analysis of multichannel electrogastrograms

Hualou Liang *

Center for Complex Systems and Brain Sciences, Florida Atlantic University, P.O. Box 3091, Boca Raton, FL 33431, USA

Received 5 October 2000; received in revised form 2 February 2001; accepted 15 February 2001

Abstract

The electrogastrogram (EGG), a cutaneous measurement of gastric electrical activity, can be severely contaminated by endogenous biological noise sources such as respiratory signal. Therefore it is important to establish effective artifact removal methods. In this paper, a novel blind signal separation method with a flexible non-linearity is introduced and applied to extract the gastric slow wave from multichannel EGGs. Simulation results show that our algorithm is able to separate a wide range of source signals, including mixtures of Gaussian sources. On real data, we demonstrate the successful applications of our procedure to extract the gastric slow wave from multichannel EGGs. As a result, the extracted clean gastric slow wave can be used to facilitate further analysis, e.g. as a reference signal for multichannel adaptive enhancement of the EGG. © 2001 IPEM. Published by Elsevier Science Ltd. All rights reserved.

Keywords: Electrogram; Stomach; Blind source separation; Independent Component Analysis

1. Introduction

The electrogastrogram (EGG), a cutaneous measurement of gastric myoelectrical activity, can be recorded by placing electrodes on the abdominal skin. Its main component, gastric slow wave or basic electrical rhythm, has a frequency of 3 cycles/min (3 cpm) in healthy humans. Due to its noninvasiveness and recent advances in methodology, EGG has become an attractive tool for diagnosis and treatment of gastric dysrhythmia, and for electrophysiological studies of the stomach [1–4].

Unlike other surface electrophysiological measurements such as electrocardiograph (ECG), however, the clinical applications of this non-invasive method have been limited [4–7]. One of the main problems with the EGG is the poor quality of the recording, i.e., the weakness of the real gastric signal and the strong interference such as respiratory artifact and random noise. As a result, direct visual analysis of the EGG is impossible. Several methods have been designed and applied to improve the quality of the EGG including bandpass filtering [8,9],

fast Fourier transform [10,11], phase-lock filtering [12], autoregressive modeling [13], adaptive filtering [14–16] and neural networks [17]. More recently, a neural network-based blind signal separation method [18] has shown its efficiency for separation of the gastric signal from noisy EGG recordings.

In this paper, a novel blind signal separation method called adaptive independent component analysis (ICA) is presented. In contrast to the previous algorithm [18], our method substantially differs in two aspects. First, instead of only using the fourth-order statistic or kurtosis of the signals, we use all higher-order statistics of the signals. Specifically, the separation is achieved under a maximum likelihood framework by considering a simple parametric model that is constructed with a family of exponential power density functions. As a result, an explicit algorithm for the adaptation of the non-linearity to various marginal densities in ICA is derived. Thus, the signal separation can be obtained without any precise knowledge of their probability distribution.

Second, theoretical considerations as well as empirical observations [19] have shown that applying *fixed* nonlinearity to all the source signals is limited to separating sources with super-Gaussian distributions, i.e. sources having sharply peaked probability density functions

* Tel.: +1-561-297-0108; fax: +1-561-297-3634.

E-mail address: liang@walt.ccs.fau.edu (H. Liang).

(pdf) with heavy tails. In reality, the source signals may have various distributions such as super-Gaussian, Gaussian and sub-Gaussian (negative kurtosis). The ICA with fixed nonlinearity can therefore find independent signals which are not the underlying sources. In other words, the ICA may contrive to find statistically independent signals at the cost of physically improbable solutions. In our method, we place additional constraint by using *adaptive* non-linearity function to match various possible signal distributions, and may therefore be widely applicable.

The aims of the present report are therefore twofold. First to develop a general blind source separation method under a maximum likelihood framework. Second to apply the proposed method to extract the gastric slow wave from multichannel EGGs. Computer simulations are first conducted to illustrate that our technique is able to capture some salient features of the underlying signal distribution, enabling separation of mixture of Gaussian sources which usually may not be separated by other algorithms. Real world applications to multichannel EGG signal separation are further demonstrated.

Preliminary reports of some of the results described here were presented in Ref. [20].

2. Methods

2.1. The measurement of the EGG

The EGG data used in this study were obtained from ten healthy subjects with body mass index of 18–37 kg/m². The study protocol was approved by the Human Subjects Committee at the University of Kansas Medical Center, and written consent forms were obtained from all subjects before the study. Gastric myoelectrical activity was recorded in each subject for at least 30 minutes in the fasting state using a custom-made 4-channel device (Sandhill Scientific, Inc., Highlands Ranch, CO). The device consisted of four identical amplifiers, each with cut-off frequencies of 1.0 and 18.0 cpm. Prior to the placement of electrodes, the abdominal surface where the electrodes were to be positioned was shaved if hairy, and cleaned with sandy skin-prep paste (Omini Prep, Weave and Co., Aurora, CO) to reduce the impedance. Six silver/silver chloride electrodes (VER MED, Bellow Falls, VT) were placed on the abdominal skin over the stomach, including four active electrodes 1–4, one common reference electrode 0 and a ground electrode. Electrode 3 was placed at the midpoint between xiphoid process and navel, electrode 4, 4 cm to subject's right horizontal to electrodes 3; electrodes 2 and 1 were positioned 45° upper left to electrode 3 with an interval of 4 cm. Electrode 0 was placed 6–8 cm right horizontal to electrode 1. Four channel EGG recordings were derived by connecting each of the active electrodes to

the common reference electrode. On-line digitization with a sampling frequency of 4 Hz was performed using an analog-to-digital converter installed on the recorder and digitized samples were stored on the recorder. The subjects were in a supine position and instructed not to talk and to remain as still as possible during the recording to avoid motion artifacts.

2.2. Adaptive ICA

Independent component analysis, which has enjoyed recent theoretical [19,21–24] and experimental [18,25] attention, refers to the recovery of a set of statistically independent sources when only mixtures of these sources with unknown coefficients are observed. Consider unknown source signals $s_i(t), i=1, \dots, n$ which are mutually independent, and can be gastric slow waves, respiratory artifact and line noise etc. The mixture of the sources of the sensor output $\mathbf{x}(t)$, multichannel EGG recording in our case, can be described by

$$\mathbf{x}(t) = \mathbf{A}\mathbf{s}(t) \quad (1)$$

where $\mathbf{A} \in \mathbf{R}^{n \times n}$ is an unknown non-singular mixing matrix, $\mathbf{s}(t) = [s_1(t), \dots, s_n(t)]^T$ and $\mathbf{x}(t) = [x_1(t), \dots, x_n(t)]^T$.

Without knowing the source signals and the mixing matrix, we want to recover the original signals from the observations $\mathbf{x}(t)$ by the following linear transform:

$$\mathbf{u}(t) = \mathbf{W}\mathbf{x}(t) = \mathbf{W}\mathbf{A}\mathbf{s}(t) \quad (2)$$

where $\mathbf{u}(t) = [u_1(t), \dots, u_n(t)]^T$ is an estimate of the sources and $\mathbf{W} \in \mathbf{R}^{n \times n}$ is a separating matrix. The sources are exactly recovered when \mathbf{W} is the inverse of \mathbf{A} , i.e. $\mathbf{W} = \mathbf{A}^{-1}$. After a possible permutation and scale change, we get the performance matrix \mathbf{P} ,

$$\mathbf{P} = \mathbf{W}\mathbf{A} \quad (3)$$

so that if \mathbf{P} is normalized and reordered a perfect separation leads to the identity matrix.

The basic idea of ICA in term of maximum likelihood is to model the observation \mathbf{x} as being generated from latent variables \mathbf{s} via a linear mapping \mathbf{A} . The likelihood of the data set in the given model is a function of the model's parameters. In the noiseless case, we can use a parametric density estimator $\hat{p}(\mathbf{x}; \mathbf{a})$ to find the parameter vector \mathbf{a} that minimizes the difference between the generative model $\hat{p}(\mathbf{x}; \mathbf{a})$ and the observed distribution $p(\mathbf{x})$. Note that each vector \mathbf{a} can be considered as a basis vector of the matrix \mathbf{A} so that $\hat{p}(\mathbf{x}; \mathbf{a})$ is an estimate of the observed vector $p(\mathbf{x})$. An appropriate difference between the estimate and the observation can be measured using the Kullback–Leibler (KL) divergence [24], D :

$$D(p(\mathbf{x}), \hat{p}(\mathbf{x}; \mathbf{a})) = \int p(\mathbf{x}) \log \frac{p(\mathbf{x})}{\hat{p}(\mathbf{x}; \mathbf{a})} d(\mathbf{x}) \quad (4)$$

$$=H(\mathbf{x})-\int p(\mathbf{x})\log\hat{p}(\mathbf{x};\mathbf{a})d\mathbf{x}$$

where $p(\mathbf{x})$ is the pdf of the observation \mathbf{x} and $\hat{p}(\mathbf{x};\mathbf{a})$ is a parametric estimate of the distribution $p(\mathbf{x})$. The divergence $D(p(\mathbf{x}), \hat{p}(\mathbf{x};\mathbf{a}))$ is zero only if our estimate $\hat{p}(\mathbf{x};\mathbf{a})$ matches the observation $p(\mathbf{x})$. The normalized log-likelihood of $\hat{p}(\mathbf{x};\mathbf{a})$ is therefore:

$$L=\frac{1}{T}\sum_{t=0}^T\log\hat{p}(\mathbf{x}_t;\mathbf{a}) \quad (5)$$

where T is the number of observations of \mathbf{x} .

To obtain a maximum likelihood algorithm we find the gradient of the log likelihood through applying a stochastic gradient optimization. By introducing $\mathbf{W}=\mathbf{A}^{-1}$ the log-likelihood for a single observation \mathbf{x} is given [24] by

$$\log p(\mathbf{x}|\mathbf{W})=\log \det \mathbf{W}+\sum_i \log p_i(W_{ij}x_j) \quad (6)$$

We then obtain the following formula,

$$\frac{\partial D}{\partial \mathbf{W}}=-\mathbf{W}^{-T}-\frac{p'_i}{p_i}\mathbf{x}^T \quad (7)$$

Setting the $p_i(u_i)$ to the derivative of the activation function of a logistic function, the algorithm reduces to that described in [19]. Since the entropy of \mathbf{x} , $H(\mathbf{x})$ is not dependent on \mathbf{W} , maximizing the log likelihood is minimizing the KL divergence:

$$\frac{\partial L}{\partial \mathbf{W}}=-\frac{\partial D}{\partial \mathbf{W}}=\mathbf{W}+\frac{p'_i}{p_i}\mathbf{u}^T\mathbf{W} \quad (8)$$

In the above formula natural or relative gradient [21] is used to enhance the computational efficiency.

When calculating the likelihood, an open question is how to select the form of the activation function so that it can match input's pdf. In other words, this is how to choose the marginal density functions, $p_i(u_i)$, which in practice, however, are not known. Here we consider a family of exponential power density functions to be our set of basis function:

$$p_\alpha(x)=c_1\exp(c_2|x|^\alpha) \quad (9)$$

where α is a positive constant, and c_1, c_2 , are normalization constants that ensure that $p_\alpha(x)$ is a probability density of unit variance. The width of the distribution is controlled by c_2 , and the weight of its tails is determined by α . When α is set to different values, we obtain different densities which range from super-Gaussian (positive kurtosis) to sub-Gaussian (negative kurtosis). For

example, p is Gaussian when $\alpha=2$. Thus the densities in this family can be used as examples of different non-Gaussian densities. This is why we choose this set of the non-linearity function.

An alternative to the parametric density model above, which may also be used for the separation of sub- and super-Gaussian sources, can be defined by

$$p(x)=\mu\varphi(x)+(1-\mu)c\varphi(c(x-1)) \quad (10)$$

where c is constant, and μ is a parameter that takes all the values in the interval $0\leq\mu\leq 1$, $\varphi(x)$ is the Gaussian function. In fact, this is the case of mixtures of Gaussian, which was discussed in [26]. This family includes asymmetric densities of both negative and positive kurtosis. Only the exponential power family of density functions will be considered in this context. Similar derivation should be obtained for Gaussian mixture densities.

The normalized log likelihood is

$$L=\frac{1}{T}\sum_{t=1}^T\log p_\alpha(x)=\log c_1+c_2|x|^\alpha \quad (11)$$

To learn the parameter α , for example, we need the derivative

$$\frac{dL}{d\alpha}=c_2|x|^\alpha\log|x| \quad (12)$$

To compute the parameters c_1, c_2 , and α of L (see Eq. (11)) and update \mathbf{W} (see Eq. (8)), schemes based on the natural gradient algorithm [21] and the quasi-Newton method can be used. The simulation given below is based on the quasi-Newton method, in which the precision required of the objective function of minimizing $-\log L$ is set to 10^{-6} and the maximum number of iterations is 100. Here the precision is defined as the absolute difference between the objective function values of two successive steps.

3. Results

In order to evaluate the performance of our approach, both the computer simulation and EGG applications are given below. First, we simulate it on computer using synthetic source signals and random mixing matrix. Second, we demonstrate the ability of the proposed algorithm to extract the gastric slow wave from multi-channel EGGs. All the experiments were performed under MATLAB 5.2 for Linux.

3.1. Decomposition of simulated data

Six synthetic source signals, including both sub-Gaussian, super-Gaussian and Gaussian, were generated and

randomly mixed. It should be noted, unlike the source signals used in other experiments that usually consist of only *one* Gaussian [22,27], we use two Gaussian. The first 100 values of the source signals, whose total length was 2000 points, are depicted in Fig. 1. From top to bottom of the left column, there are two sub-Gaussian, two super-Gaussian and two Gaussian respectively. The mixed signals are plotted in the middle column, and the separation result is shown in the right column. We can see from Fig. 1 that the separated signals (right column) match the source ones (left column) quite well.

But one question still remains open — what should the criteria be for two Gaussian signals to be considered as separated. To address this question we calculate the correlation coefficients between source signals and separated ones, which are given by the following matrix,

$$\begin{bmatrix} -0.004 & 0.038 & -0.002 & \mathbf{0.999} & 0.004 & 0.001 \\ 0.069 & -0.028 & \mathbf{-0.997} & 0.0004 & 0.001 & 0.0002 \\ \mathbf{0.999} & -0.007 & 0.046 & 0.003 & -0.011 & 0.003 \\ -0.030 & \mathbf{-0.997} & 0.036 & 0.052 & -0.037 & 0.010 \\ -0.046 & 0.064 & 0.008 & 0.010 & \mathbf{-0.997} & 0.007 \\ 0.007 & -0.009 & -0.003 & -0.032 & -0.016 & \mathbf{-0.999} \end{bmatrix}$$

It can be seen from the above source correlation matrix that the good separation is achieved by our method.

The performance of the algorithm can also be examined in another way. Fig. 2 shows the performance matrix \mathbf{P} as indicated in Eq. (3). If the separation is per-

fect, the result will be a ridge along the diagonal with all off-diagonal elements close to zero. Indeed, \mathbf{P} is approximately the identity matrix which indicates nearly perfect separation.

3.2. Applications to EGG data

Fig. 3(a) shows 10-min 2-channel EGG data from a healthy human subject. The separation by the proposed method is shown in Fig. 3(b), from which we can see the noise-free gastric slow wave signal (channel 1) is well separated from noise contaminations, such as respiratory and random noise.

A further application example is illustrated in Fig. 4, where 10-min three-channel EGG recordings collected from a healthy subject are plotted in Fig. 4(a), the separation results are shown in Fig. 4(b). Comparing the original recordings in Fig. 4(a) with the separated signals in Fig. 4(b), we can see that the gastric slow wave with about 3 cpm (channel 1 in Fig. 4(b)) is clearly extracted, whereas the respiratory and random noise are concentrated on the channel 2 and 3.

To verify the extracted gastric slow wave is indeed the *true* component of gastric myoelectric activity, we performed cross-spectral density estimation of the extracted EGG and one of the EGG recordings using Welch's averaged periodogram method [28]. The result shows that these two signals are well correlated at the peak of 3 cpm, which is illustrated in Fig. 5. This cross-spectral analysis confirmed that our technique is able to extract the physically realistic signals.

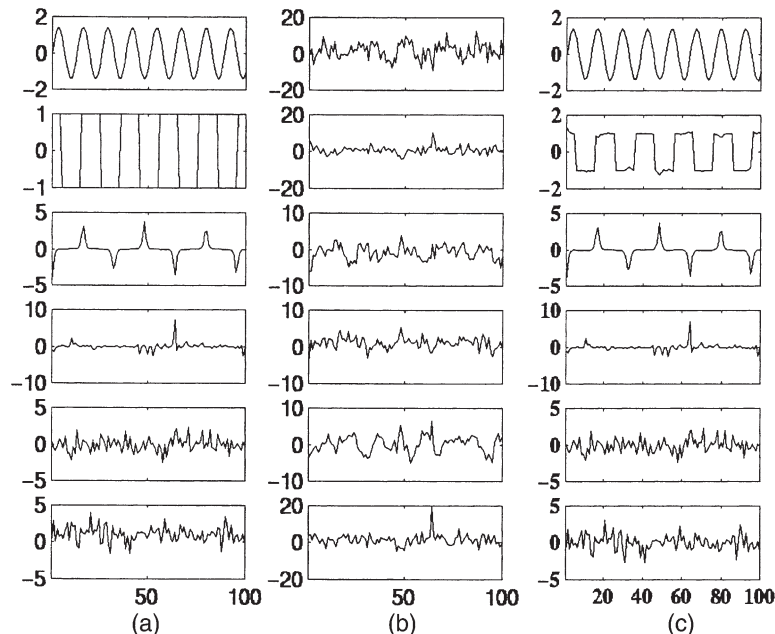


Fig. 1. Example of separation of independent source signals. (a) The sources from top to bottom consisting of two sub-Gaussian, two super-Gaussian and two Gaussian respectively. (b) The set of random mixtures of source signals in (a). (c) Estimates of the source signals.

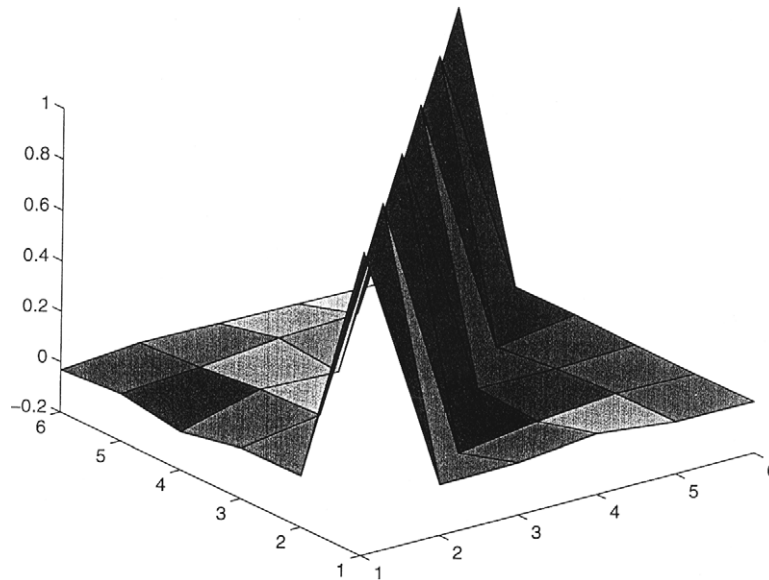


Fig. 2. Performance matrix for the separation of six sources. A ridge along the diagonal with all off-diagonal elements close to zero indicates a good separation.

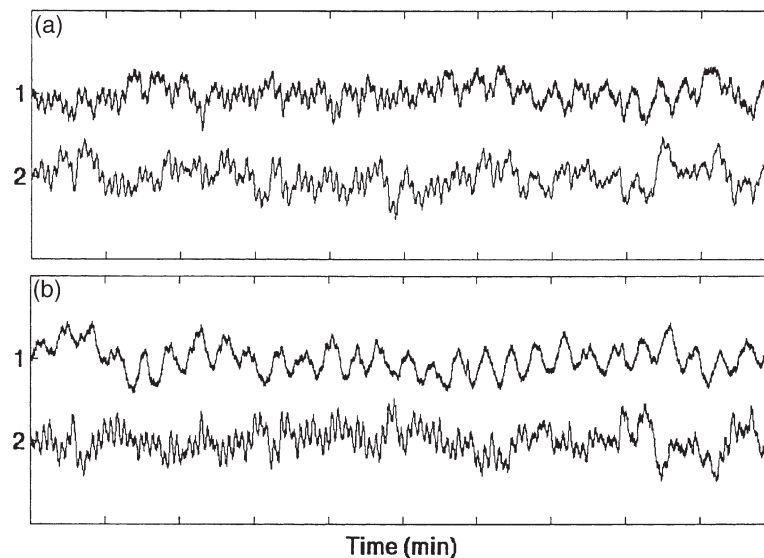


Fig. 3. Application to 2-channel EGG data. (a) Two channels raw EGG recordings. (b) Two separated signals. Channel 1 corresponds to 3 cpm gastric slow wave, channel 2 is noise contaminations.

4. Discussion and conclusions

A novel blind signal separation method with a flexible non-linearity is presented and successfully applied to extract the gastric slow wave from multichannel EGGs. A key feature of our method is the addition of prior knowledge in the form of *adaptive* non-linearity in order to match various possible signal distributions which leads to extracting physically meaningful signals. The proposed method was initially tested in a series of computer simulations, showing very good performance in the separation of signals from their linear mixtures. In experimental data obtained from human subjects, the

method was able to extract gastric slow wave from multichannel EGGs. As a consequence, the extracted clean gastric slow wave can be used as a reference signal for multichannel adaptive enhancement of the EGG.

This technique seems to be an improvement to the traditional artifact canceling methods. Adaptive filtering technique [14–16] in either time domain or transform domain has been shown to improve the quality of the EGG or to extract relevant information from the EGG. An inherent weakness of this method, however, is requiring a reference signal that is the comprehensive signal of the various artifacts to be removed. Also, the proposed method is quite different from the filtering in the fre-

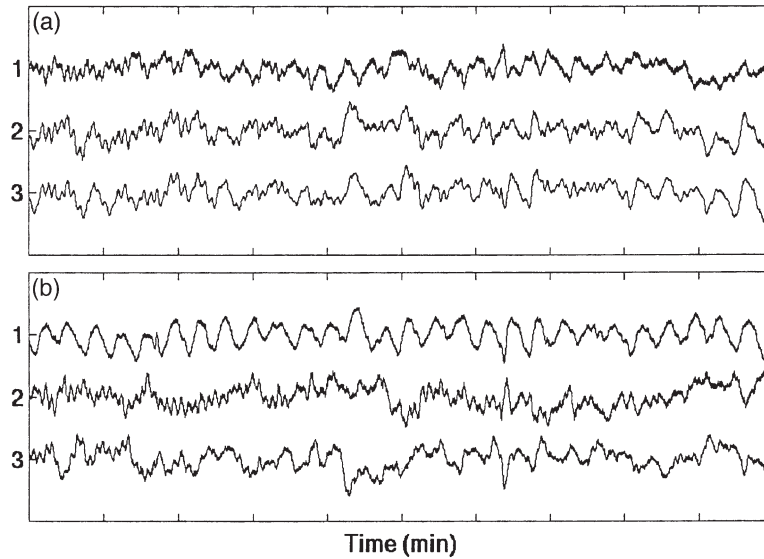


Fig. 4. Application to 3-channel EGG data. (a) Original three channels EGG recordings. (b) Three components extracted from raw EGGs. Channel 1 corresponds to 3 cpm gastric slow wave.

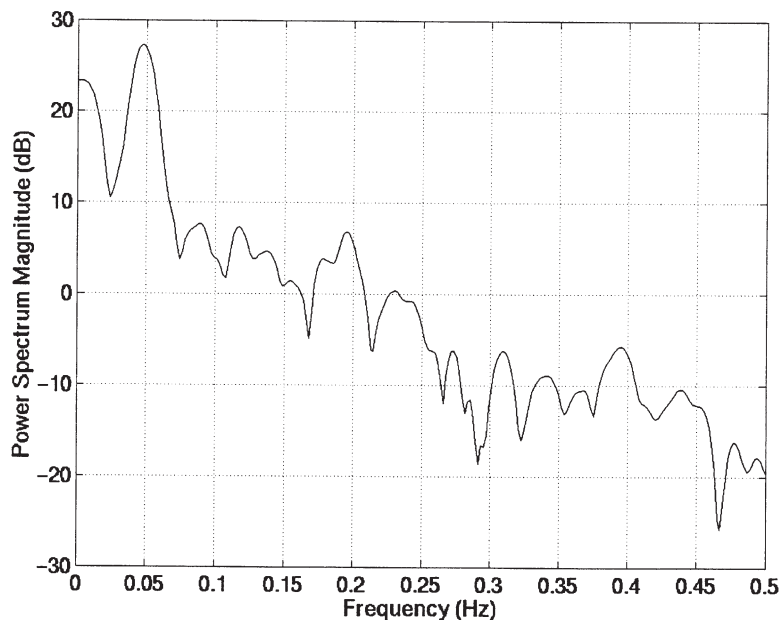


Fig. 5. The cross-spectrum of the extracted gastric slow wave and the first channel of original EGG recordings. We can see these two signals are well correlated at the peak of 3 cpm, which confirmed that our technique is able to extract the physically realistic signal.

frequency domain that is in general a compromise between preserving the signal and rejecting the noise. Particularly in case the frequency of real gastric signal can be very close to or maybe even overlaps with that of the respiratory artifact during some abnormal activities of the stomach, frequency domain filtering will fail to remove this kind of artifact. The proposed ICA method does not have such limitations, therefore is more promising and pragmatic in real world applications.

It should be noted that the basic assumption made on the data used in the proposed method is that the EGG is

a linear mixtures of a number of temporally independent sources such as gastric slow wave, small bowel signal, respiration and random noise, which is generally compatible with EGG studies [2]. In most cases this independence is verified due to the differences in physiological origins of those signals. However it may fail to remove motion artifacts from the EGG because the occurrence of motion artifacts is discontinuous. Apart from this, the algorithm implicitly requires the number of channels to be the same or greater than the number of sources. Despite these limitations, the algorithm presented here

should be applicable to other biomedical signals where both sub-Gaussian and super-Gaussian sources need to be separated without additional prior knowledge of their statistical properties.

In summary, we have formulated ICA within the framework of maximum likelihood, in which a novel blind signal separation method with a flexible non-linearity is developed. Extensive computer simulations show our approach allows to separate a wide variety of sources ranging from sub-Gaussian to super-Gaussian, and even the mixture of Gaussian provided only that they have distinct spectra. The success of our procedure is further demonstrated on real world applications to EGG signal separation. We believe that the successful application of the ICA method shown in this paper will facilitate research on the EGG.

Acknowledgements

The author would like to thank Prof. Z. Y. Lin for his technical assistance and for the data used in this paper.

References

- [1] Alvarez WC. The electrogastrogram and what it shows. *JAMA* 1922;78:1116–8.
- [2] Chen J, McCallum RW. Electrogastrogram: measurement, analysis and prospective applications. *Med Bio Eng Comput* 1991;29:339–50.
- [3] Faniloni BO, Kingma YJ, Bowes KL. Non-invasive assessment of human gastric motor function. *IEEE Trans Biomed Eng* 1987;34:30–6.
- [4] Koch KL, Stern RM, Stewart WR, Vasey MW. Electrogastrography: current issues in validation and methodology. *Psychophysiology* 1987;24:55–64.
- [5] Chen JDZ, McCallum RW. Clinical application of electrogastrogram. *Am J Gastroenterol* 1993;88:1324–36.
- [6] Mintchev MP, Kingma YJ, Bowes KL. Accuracy of cutaneous recordings of gastric electrical activity. *Gastroenterology* 1993;104:1273–80.
- [7] Verhagen MAMT, Schelven LJV, Samsom M, Smout AJPM. Pitfalls in the analysis of electrogastrographic recordings. *Gastroenterology* 1999;117:453–60.
- [8] Nelsen TS, Kohatsu S. Clinical electrogastrography and its relationship to gastric surgery. *Am J Surg* 1968;116:215–22.
- [9] Stoddard CJ, Smallwood RH, Duthie HL. Electrical arrhythmias in the human stomach. *Gut* 1981;22:705–12.
- [10] Brown BH, Smallwood RH, Duthie HL, Stoddard CJ. Intestinal smooth muscle electrical potentials recorded from surface electrodes. *Med Biol Eng Comput* 1975;13:97–103.
- [11] van der Schee EJ, Grashuis JL. Running spectrum analysis as an aid in the representation and interpretation of electrogastrographic signals. *Med Biol Eng Comput* 1987;25:57–62.
- [12] Smallwood RH. Analysis of gastric electrical signals from surface electrodes using phaselock techniques. *Med Biol Eng Comput* 1978;16:507–18.
- [13] Linkens DA, Datardina SP. Estimation of frequencies of gastrointestinal electrical rhythms using autoregressive modeling. *Med Biol Eng Comput* 1978;16:262–8.
- [14] Chen J, Lin ZY. Comparison of adaptive filtering in time-, transform- and frequency-domain: an Electrogastrographic study. *Ann Biomed Eng* 1994;22:423–31.
- [15] Chen J, Vandewalle J, Sansen W, Vantrappen G, Janssens J. Multi-channel adaptive enhancement of human electrogastrogram. *IEEE Trans Biomed Eng* 1990;37:285–95.
- [16] Kentie MA, van der Schee ET, Grashuis JL, Smout AJPM. Adaptive filtering of canine electrogastrographic signals-Part I: system design. *Med Biol Eng Comput* 1981;19:759–64.
- [17] Liang J, Cheung JY, Chen JDZ. Detection and deletion of motion artifacts in electrogastrogram using feature analysis and neural networks. *Ann Biomed Eng* 1997;25:850–7.
- [18] Wang ZS, Cheung JY, Chen JDZ. Blind separation of multichannel electrogastrograms using independent component analysis based on a neural network. *Med Biol Eng Comput* 1999;37:80–6.
- [19] Bell A, Sejnowski T. An information-maximization approach to blind separation and blind deconvolution. *Neural Comput* 1995;6:1129–59.
- [20] Liang H, Logothetis NK. Blind signal separation with a flexible non-linearity. *Proc of Int Conf Neural Inform Processing*. Japan: IOS Press, Inc, 1998:478–481.
- [21] Amari S, Cichocki A, Yang H. A new learning algorithm for blind signal separation. In: *Advances in Neural Information Processing Systems 8*. Cambridge: MIT Press, 1996:757–763.
- [22] Comon P. Independent component analysis, a new concept? *Signal Processing* 1994;36:287–314.
- [23] Jutten C, Herault J. Blind separation of sources, Part I: an adaptive algorithm based on neuromimetic architecture. *Signal Processing* 1991;24:1–10.
- [24] Pearlmutter BA, Parra LC. A context-sensitive generalization of ICA. *Proc of Int Conf Neural Inform Processing*, 1996:151–157.
- [25] Makeig S, Jung TP, Bell AJ, Ghahremani D, Sejnowski TJ. Blind separation of auditory event-related brain responses into independent components. *Proc Natl Acad Sci USA* 1997;94:10979–84.
- [26] Xu L, Cheung C, Yang H, Amari S. Maximum equalization by entropy maximization and mixture of cumulative distribution functions. *IEEE Proc Int Conf Neural Netw*, Houston, 1997:1821–1826.
- [27] Cardoso J, Souloumiac A. Blind beamforming for non Gaussian signal. *IEE Proc-F* 1993;140:362–70.
- [28] Oppenheim A, Schaffer R. *Digital Signal Processing*. New Jersey: Prentice-Hall, 1975.